

A-site disorder induced collapse of charge-ordered state and phase separated phase in manganites

K. F. Wang,^{a),b)} F. Yuan, and S. Dong

Laboratory of Solid State Microstructures, Nanjing University, Nanjing 210093, China

D. Li and Z. D. Zhang

International Center for Materials Physics, Chinese Academy of Sciences, Shenyang 110015, China
and Institute of Metal Research, Chinese Academy of Sciences, Shenyang 110016, China

Z. F. Ren

Department of Physics, Boston College, Chestnut Hill, Massachusetts 02467

J.-M. Liu^{a)}

Laboratory of Solid State Microstructures, Nanjing University, Nanjing 210093, China
and International Center for Materials Physics, Chinese Academy of Sciences, Shenyang 110015, China

(Received 26 June 2006; accepted 13 October 2006; published online 29 November 2006)

The effects of A-site cation size mismatch (A-site disorder) on the stability of charge-ordered states and phase separated phase in a series of manganites with constant A-site ionic average radii $\langle r_A \rangle = 1.18 \text{ \AA}$ but different A-site ionic size mismatches σ^2 are experimentally investigated. It is revealed that the charge/orbital ordered antiferromagnetic ground state becomes destabilized and eventually collapses into coexisting of the predominant ferromagnetic metal (FMM) state and short-range charge/orbital ordered state with increasing σ^2 , resulting in enhanced colossal magnetoresistance. However, further increasing A-site disorder will suppress the FMM state and seem to favor a cluster-glass insulating state due to the severe electronic localization. © 2006 American Institute of Physics. [DOI: 10.1063/1.2397550]

Fascinating phenomena such as colossal magnetoresistance (CMR) and charge/orbital ordered (CO–OO) states observed in doped manganites have been attracting attentions.^{1–4} This CO–OO state can be destabilized by external stimuli, such as large magnetic field, giving rise to FMM state.⁴ Moreover, the CO–OO phase and the contrasting FMM phase are found to be very close in energy.^{4–7} So the CO–OO phase can be weakened, and coexisting FMM and CO–OO states can be created by introducing some Mn-site substitution.^{7,8} Such diverse behaviors arise from strong interplay of charge, orbital, and spin orderings.^{5,6} The Mn-site doping will introduce disorder and produce the simultaneous presence of contrasting ordered phases (i.e., phase separated state) and enhance the fluctuation of the competition orders.^{6–8}

However, the Mn-site doping will introduce extrinsic effects such as the changing of carrier concentration and some magnetic impurity. Previous studies^{9–12} showed that the A-site cation size mismatch can lead to random local lattice distortion, and these disorder effects can be described by the variance of the A-site cation radius distribution expressed by $\sigma^2 = \sum_i (x_i r_i^2 - \langle r_A \rangle^2)$, where x_i and r_i are the atomic fraction and ionic radii of i -type ions at A site, respectively. This kind of A-site disorder maybe a more direct and purified road map to understand the physical mechanism and disorder effects in manganites. In Tomioka and Tokura's study, they found that the A-site disorder has great effects on the properties of manganites and gave the phase diagram of disorder versus $\langle r_A \rangle$.¹¹ However, no much data on phase separation behaviors associated with the A-site disorder are available so far. In this letter, the A-site disorder effects on the stability of CO–OO

state will be studied carefully by preparing a series of manganites which have the same A-site cation average radius $\langle r_A \rangle = 1.18 \text{ \AA}$ but with different values of σ^2 , given the same Mn-site cation, noting that manganites with $\langle r_A \rangle = 1.18 \text{ \AA}$ usually offer the CO–OO ground state at low temperature.

In our experiments, we prepared a series of samples with different variance σ^2 from 0.000 02 to 0.0078 \AA^2 , as shown in Table I. Both the $\langle r_A \rangle$ and σ^2 were calculated using standard nine-coordinated cation radii.¹³ These samples were sintered by the conventional solid-state reaction in air. High-resolution x-ray diffraction (XRD) with Cu $K\alpha$ radiation was performed on these samples at room temperature. The transport behaviors, magnetizations under zero-field cooling (ZFC), and field cooling (FC) were measured as a function of temperature T and magnetic field H using a Quantum Design superconducting quantum interference device magnetometer. The magnetic loops from $H=0$ to 7 T were recorded at 3 K. The XRD patterns of all the samples can be indexed with a single orthorhombic structure with space group $Pnma$. There is no measurable peak shift for all these samples, indicating essentially the same lattice parameters for all the samples with different disorders.

However, the samples with different disorders exhibit distinct transport behavior. The curves of zero-field resistivity (ρ) as a function of T for all the samples are plotted in Fig. 1(a). It is clearly shown that ρ is very much σ^2 dependent. Sample $\text{Pr}_{0.55}\text{Ca}_{0.45}\text{MnO}_3$ with small $\sigma^2 = 0.000 02 \text{ \AA}^2$ exhibits insulating behavior over the whole T range because of the CO–OO state. The increasing of σ^2 , i.e., increasing A-site disorder, leads to rapid decreasing of ρ , as shown in Fig. 1(b) at $T=3 \text{ K}$. Moreover, the samples with $\sigma^2 = 0.0004$ and 0.0025 \AA^2 possess metallic ground state and exhibit metal-insulator transition with increasing T , which is popular in CMR manganites. However, when σ^2 increases

^{a)} Author to whom correspondence should be addressed.

^{b)} Electronic mail: wangkf@nju.edu.cn

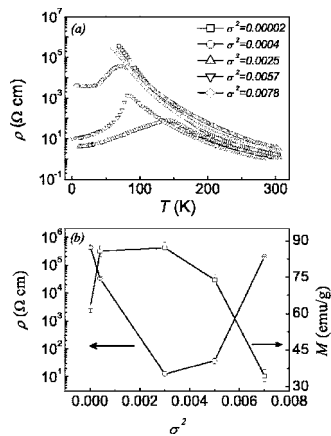


FIG. 1. (a) Measured ρ - T relations for the samples with σ^2 from 0.000 02 to 0.0078 \AA^2 ; (b) σ^2 dependences of M measured at $T=3$ K under $H=3$ T and σ^2 dependences of zero field ρ measured at $T=50$ K.

further, ρ increases again, and the sample $\text{Gd}_{0.55}(\text{Ca}_{0.3}\text{Sr}_{0.7})_{0.45}\text{MnO}_3$ with $\sigma^2=0.0078$ \AA^2 becomes insulating again over the whole T range.

In order to reveal the magnetic properties in systems of different σ^2 , we turn to the magnetic behaviors of these samples. Figure 2 shows the T dependence of the dc magnetization M for samples with $\sigma^2=0.000$ 02, 0.0025, 0.0057, and 0.0078 \AA^2 , respectively. The sample $\text{Pr}_{0.55}\text{Ca}_{0.45}\text{MnO}_3$ with the smallest σ^2 exhibits a CO–OO transition at $T_{\text{CO}} \sim 227.5$ K, and subsequently an antiferromagnetic (AFM) transition at $T_N \sim 112.5$ K, consistent with previous research.¹⁴ The increasing A -site disorder significantly affects the magnetic behavior. The samples with a larger $\sigma^2 = 0.0004$, 0.0025, and 0.0057 \AA^2 exhibit the paramagnetic-ferromagnetic (FM) transitions which accompany with the insulator-metal transitions in transport behavior. However, the Curie temperature firstly increases from $T_C \sim 109.1$ K at $\sigma^2=0.0004$ to ~ 162.1 K at $\sigma^2=0.003$, and then decreases to ~ 114.3 K with further increasing of σ^2 to 0.0057 \AA^2 , consistent with the transport measurements. As σ^2 further increases to 0.007, the M - T curve at ZFC case shows a cusp-like peak at about $T=T_f \sim 47$ K. Moreover, the curve at FC case does not have a cusp and increases straightly. Obviously, there is a significant irreversibility between the ZFC and FC magnetization curves in low T range. Such an irreversibility is one of the typical features of cluster-glass-like state in phase separated manganites.^{15,16}

To investigate the magnetic ground state, the H dependences of M at $T=3$ K shown in Fig. 3 for samples of $\sigma^2 = 0.000$ 02, 0.0004, 0.0025, and 0.007 \AA^2 , were measured. It is clearly shown that for sample with $\sigma^2=0.000$ 02 \AA^2 , M exhibits a moderate jump at $H \sim 6$ T, but remains unsaturated even to 7 T. At $\sigma^2=0.0004$ \AA^2 , the saturated M is not achieved until $H \sim 3$ T, at which a stepwise behavior occurs.

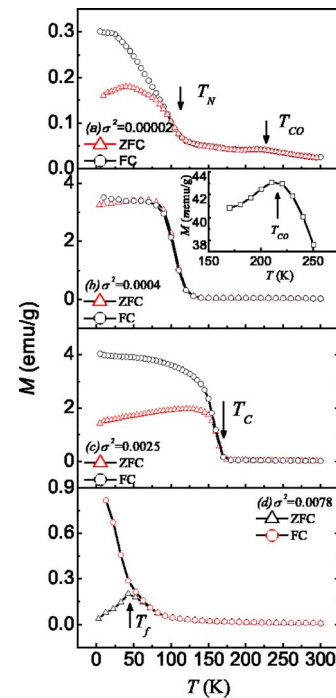


FIG. 2. (Color online) Measured M - T relations under ZFC and FC conditions for the samples with (a) $\sigma^2=0.000$ 02 \AA^2 , (b) 0.0004 \AA^2 , (c) 0.0025 \AA^2 , and (d) 0.0078 \AA^2 . The arrows in (d) indicate the cluster-glass transition point. The inset in (b) is the part of the CO–OO transition, as described in text.

Afterwards, the magnetization becomes saturated. For the samples with higher $\sigma^2=0.0025$ and 0.0057 \AA^2 , the saturated M is achieved at a very low $H \sim 1$ T, indicating a FM ground state. However, M of the sample with the highest $\sigma^2 = 0.0078$ \AA^2 does not saturate even at a field as high as $H = 7$ T. These effects immediately allow us to argue a possible cluster-glass-like transition occurring at T_f for those samples of large σ^2 .

Based on all of the results presented above, we may conclude that upon increasing A -site disorder, i.e., increasing of σ^2 from 0.000 02 to 0.0025 \AA^2 , the CO/OO ground state is gradually suppressed and the ground state changes to a FMM state. But further increasing of the disorder ($\sigma^2 > 0.0025$ \AA^2) suppresses the FMM ground state either, and ultimately leads to the cluster-glass insulating ground state.

To understand the physics underlying the collapse of the CO–OO state, one may consider the scenario of phase separation in response to the A -site disorder and magnetic field. It was revealed that the A -site cationic size mismatch (described by σ^2), as well as the A -site cationic mean radius $\langle r_A \rangle$ controls the properties of manganites.^{2,9–12} When σ^2 is large, the A -site ions randomly distribute in the lattice, which keeps the macroscopic structure unchanged, but the size difference

TABLE I. Summary of chemical, structural, and physical data for the $\text{RE}_{0.55}\text{AE}_{0.45}\text{MnO}_3$ series with A -site cation mean radius $\langle r_A \rangle \sim 1.48$ \AA .

Composition	$\langle r_A \rangle$ (\AA)	σ^2 (\AA^2)	T_{CO} (K)	T_C (K)	T_f (K)	M (μ_B pfu)
$\text{Pr}_{0.55}\text{Ca}_{0.45}\text{MnO}_3$	1.179	0.000 02	221.7	2.72
$(\text{La}_{0.25}\text{Nd}_{0.75})_{0.55}\text{Ca}_{0.45}\text{MnO}_3$	1.178	0.000 4	214.8	109.8	...	3.36
$\text{Nd}_{0.55}(\text{Ca}_{0.7}\text{Sr}_{0.3})_{0.45}\text{MnO}_3$	1.186	0.002 5	...	164.9	...	3.48
$\text{Sm}_{0.55}(\text{Ca}_{0.47}\text{Sr}_{0.53})_{0.45}\text{MnO}_3$	1.183	0.005 7	...	105.8	...	2.47
$\text{Gd}_{0.55}(\text{Ca}_{0.3}\text{Sr}_{0.7})_{0.45}\text{MnO}_3$	1.181	0.007 8	46.3	1.51

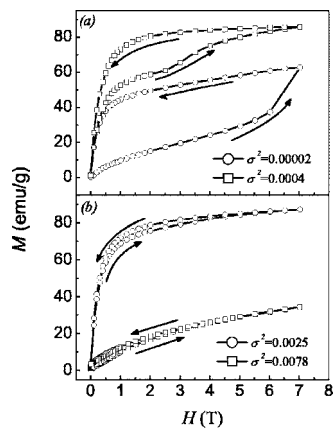


FIG. 3. Measured M - H curves at $T=3$ K, for the samples with (a) $\sigma^2=0.0002$ and 0.0004 \AA^2 , (b) 0.0025 and 0.0078 \AA^2 . The arrows indicate the variation of H during measurements.

between the neighboring A -site R^{3+} and M^{2+} ions around one oxygen ion may enable the random oxygen displacement, and consequently a local distortion of MnO_6 octahedra. The oxygen displacements and the radial distortions of the MnO_6 octahedra are randomly distributed in the system and can be regarded as disorder, which can be described by σ^2 .

The systems studied in this work have the constant $\langle r_A \rangle = 1.18 \text{ \AA}$, which is smaller than the ideal value. So the sample $\text{Pr}_{0.55}\text{Ca}_{0.45}\text{MnO}_3$ with the smallest $\sigma^2=0.0002 \text{ \AA}^2$ exhibits the CO-OO ground state.^{2,4} The increasing of σ^2 will result in some interesting effects. Firstly, a moderate A -site disorder will introduce larger A -site cations in some MnO_6 octahedra and may suppress the crystal distortion in these regions, which ultimately make these regions transit to the FMM state. In other regions the disorder will lead to the increasing of the A -site size mismatch and the local lattice distortion is enhanced. Secondly, it is argued that $\text{Pr}_{0.55}\text{Ca}_{0.45}\text{MnO}_3$ locates near the multicritical points and the competition among FMM and CO-OO ordered phases is very significant.⁶ Some experiments demonstrated that there exists the coexistence of FMM and CO-OO phases in $\text{Pr}_{0.55}\text{Ca}_{0.45}\text{MnO}_3$.^{7,17} The disorder will enhance the competition and make the system trend to one of the ordered phase.

So the slight increasing of A -site disorder, referring to $\text{Pr}_{0.55}\text{Ca}_{0.45}\text{MnO}_3$, suppresses the long-range CO-OO state but favors the FMM phase. Then the FMM phase increases and becomes predominant. In this condition the CO-OO state still survives, thus the magnetization behavior of the sample with $\sigma^2=0.0004$ exhibits a weak cusp at ~ 214.8 K, which corresponds to the weak CO-OO transition and then exhibits the FMM transition at ~ 109.8 K, as shown in Fig. 3(b) and the inset. Moreover, the M - H curve of this sample shows an evident stepwise behavior, corresponding to the field-induced destroy of the CO-OO region and the growth of the FMM phase. These effects are popular in phase separated system, demonstrates the coexistence of the CO-OO and FMM phases.^{17,18} Increasing of the A -site disorder from this stage to 0.003 makes the FMM phase increase and no CO-OO transition is observable. Correspondingly, the Curie temperature and the magnetization increase, as shown in Table I.

However, when A -site disorder increases further, the number and the strength of the random lattice distortion increase, which ultimately suppresses the FMM phase, too.^{11,12}

In the systems of $\sigma^2=0.0025-0.0057 \text{ \AA}^2$, the FMM phase is suppressed, resulting in the decreasing of the Curie temperature and the magnetization. As $\sigma^2>0.0057 \text{ \AA}^2$, it is argued that the long-range FMM and CO-OO ordering are completely broken into short-range ordered regions. This corresponds to the so-called cluster-glass state.

It should be noted that the A -site disorder influences the magnetic transport behavior of the system evidently, too. $\text{Pr}_{0.55}\text{Ca}_{0.45}\text{MnO}_3$ scarcely exhibits MR effect. But it can be seen that the samples with $\sigma^2=0.0004$, 0.0025 , and 0.0057 \AA^2 exhibit very large CMR effects and the MR ratio approaches to 100%. The reason is that the ground state of these samples is the coexisting FMM and short-range CO-OO regions. The external field will destroy the CO-OO regions and result in growth of the FMM regions, and then the enhanced CMR effects.

In conclusion, we have investigated the effect of the A -site disorder on the magnetic and transport behaviors of CO-OO manganites. It has been observed that the increasing of σ^2 breaks the CO-OO AFM state and makes the ground state changing to FMM phase, so an enhanced colossal magnetoresistant effect appears. Further increasing of σ^2 suppresses the FMM state, too. And then the ground state returns to an insulator which is denoted as a cluster-glass state. Our experimental results seem to confirm the prediction of Sen *et al.*¹⁹ and Motome *et al.*²⁰ that the disorder in manganites can induce an insulator-metal transition.

This work was supported by the National Natural Science Foundation of China (50332020, 50528203, and 10021001) and the 973 Projects of China (2006CB0L1002).

¹S. Jin, T. H. Tiefel, M. McCormack, R. A. Fastnacht, R. Ramesh, and L. H. Chen, *Science* **264**, 413 (1994).

²Myron B. Salamon and M. Jaime, *Rev. Mod. Phys.* **73**, 583 (2002).

³C. Zener, *Phys. Rev.* **82**, 403 (1951).

⁴Y. Tokura and N. Nagaosa, *Science* **288**, 462 (2000), and references therein; C. H. Chen, S. Morf, and S.-W. Cheong, *Phys. Rev. Lett.* **83**, 4792 (1999).

⁵S. Murakami and N. Nagaosa, *Phys. Rev. Lett.* **90**, 197201 (2003).

⁶Y. Tokura, *Rep. Prog. Phys.* **69**, 797 (2006).

⁷*Nanoscale Phase Separation and Colossal Magnetoresistance*, edited by E. Dagotto (Springer, Berlin, 2003), 357.

⁸D. Akahoshi, M. Uchida, Y. Tomioka, T. Arima, Y. Matsui, and Y. Tokura, *Phys. Rev. Lett.* **93**, 177203 (2003).

⁹L. M. Rodriguez-Martinez and J. Paul Attfield, *Phys. Rev. B* **54**, R15622 (1996).

¹⁰L. M. Rodriguez-Martinez and J. Paul Attfield, *Phys. Rev. B* **58**, 2426 (1998).

¹¹Y. Tomioka and Y. Tokura, *Phys. Rev. B* **70**, 014432 (2004).

¹²K. F. Wang, Y. Wang, L. F. Wang, S. Dong, H. Yu, Q. C. Li, J.-M. Liu, and Z. F. Ren, *Appl. Phys. Lett.* **88**, 152505 (2006); K. F. Wang, Y. Wang, L. F. Wang, S. Dong, D. Li, Z. D. Zhang, H. Yu, Q. C. Li, and J.-M. Liu, *Phys. Rev. B* **73**, 134411 (2006).

¹³R. D. Shannon, *Acta Crystallogr., Sect. A: Cryst. Phys., Diff., Theor. Gen. Crystallogr.* **A32**, 751 (1976).

¹⁴Y. Tomioka, A. Asamitsu, and Y. Tokura, *Phys. Rev. B* **53**, R1689 (1996).

¹⁵H. Y. Hwang, S.-W. Cheong, P. G. Radaelli, M. Marezio, and B. Batlogg, *Phys. Rev. Lett.* **75**, 914 (1995).

¹⁶J. A. Mydosh, *Spin Glasses: An Experimental Introduction* (Taylor & Francis, Washington, 1993), 102.

¹⁷Guixin Cao, Jincang Zhang, Shixun Cao, Chao Jing, and Xuechu Shen, *Phys. Rev. B* **71**, 174414 (2005).

¹⁸D. Zhu, B. Raveau, A. Maignan, M. Hervieu, V. Hardy, and C. Martin, *J. Appl. Phys.* **95**, 4245 (2004).

¹⁹C. Sen, G. Alvarez, and E. Dagotto, *Phys. Rev. B* **87**, 064428 (2004).

²⁰Y. Motome, N. Furukawa, and N. Nagaosa, *Phys. Rev. Lett.* **91**, 167204 (2003).